Life Sciences 239 (2019) 116975

Contents lists available at ScienceDirect

Life Sciences

journal homepage: www.elsevier.com/locate/lifescie

Abnormal thyroid hormone receptor signaling in osteoarthritic osteoblasts regulates microangiogenesis in subchondral bone

Lei Li[a,1], Meng Li[b,1], Yiqun Pang[c,1], Jun Wang[a], Yunpeng Wan[a], Chen Zhu[b,**], Zongsheng Yin[a,*]

[a] Department of Orthopaedics, the first affiliated hospital of Anhui Medical Universtiy, #218 Jixi Road, Hefei, Anhui, China
[b] Department of Orthopaedics, the first affiliated hospital of University of Science and Technology of China, #17 Lujiang Road, Hefei, Anhui, China
[c] Department of radiology, the first affiliated hospital of University of Science and Technology of China, #17 Lujiang Road, Hefei, Anhui, China

ARTICLE INFO

Keywords:
Osteoarthritis
Subchondral bone
Angiogenesis
Thyroid hormone receptor

ABSTRACT

Aims: Previous study indicated that the increase of local bio-availability of 3′3′5-triiodothyronine (T3) influenced osteoarthritis (OA) initiation. We aimed to investigate the role of thyroid hormone receptors (THRs) signaling in OA osteoblasts.

Materials and methods: THRs expression in OA was detected by immunohistochemistry, immunofluorescence, RT-qPCR and western blotting. These effects on the expression of angiogenesis-related factors were examined after THRα or THRβ knockdown in OA osteoblasts. Fluorescence in situ hybridization was used to confirm the leading receptor for regulating angiogenesis-related factors. Co-culture model was utilized to observe the MMPs expression in chondrocytes after THRα knockdown in osteoblasts. The *in vivo* effects were also studied after intra-articular injection with THRα siRNA in OA model mice. Micro-CT and immunohistochemistry were employed to evaluate the changes of subchondral bone.

Key findings: THRs expression and nuclear translocation were upregulated in human OA osteoblasts. Immunohistochemistry showed that angiogenic activities were increased in OA subchondral bone of human and mice. VEGF, HIF-1α and IGF-1, these THR downstream genes were downregulated after THRα knockdown in OA osteoblasts. Fluorescence in situ hybridization further indicated that THRα signaling mainly regulated VEGF expression. Intra-articular injection with THRα siRNA reduced angiogenic activities in OA model mice subchondral bone and ameliorated cartilage degradation. Micro-CT analysis displayed that the aberrant subchondral bone formation in OA was promoted.

Significance: The microangiogenesis in subchondral bone may be partly attributed to abnormal THRα signaling in osteoblasts, and local inhibition of the THRα could be a potential target to treat OA.

1. Introduction

Osteoarthritis (OA), the most common degenerative joint disease, is the leading cause of physical disability and dysfunction, which affects the aging population in the world [1]. Despite the loss of articular cartilage in OA, currently numerous studies have focused on angiogenesis at osteochondral unit and the pathological process of subchondral bone [2–4]. The crosstalk of bone-cartilage allows the transport of metalloproteinase (MMPs), inflammatory factors and chemokines, which exposes cartilage to detrimental microenvironment [5]. However, vascular invasion mainly contributed to the crosstalk and underlying mechanism remains uncertain. Subchondral bone is considered to provide the mechanical support for articular cartilage, and it also undergoes bone resorption and remodeling in response to mechanical load changes. The process of bone remodeling characterized by abnormally proliferative osteoblasts after subchondral bone marrow loss in advanced OA [6,7]. An increasing amount of studies showed that subchondral bone not only transferred mechanical pressure to the cartilage, but also synthesized and released activated cytokines to disturb cartilage metabolism in OA [8–10]. Meanwhile, the aberrant subchondral bone formation is accompanied by blood capillary invasion, suggesting a close association between osteogenesis and angiogenesis [11].

Osteoblasts, which synthesize extracellular matrix proteins to maintain skeletal homeostasis and matrix mineralization, play a pivotal

Abbreviations: OA, Osteoarthritis; T3, 3′3′5-triiodothyronine; THR, thyroid hormone receptor; MMP, Metalloproteinase; VEGF, Vascular endothelial growth factor; HIF-1α, Hypoxia-inducible factor; IGF-1, Insulin-like growth factor; siRNA, Small interfering RNA

* Corresponding author.
** Corresponding author.
E-mail addresses: zhuchen19790820@sina.com (C. Zhu), yzsahmu1961@sina.com (Z. Yin).
[1] Co-first authors.

https://doi.org/10.1016/j.lfs.2019.116975
Received 5 August 2019; Received in revised form 11 October 2019; Accepted 14 October 2019
Available online 22 October 2019
0024-3205/

role in OA pathogenesis and are involved in subchondral bone sclerosis [12]. Aside from osteoprotegerin (OPG) and nuclear factor (NF)-κB ligand (RANKL), osteoblasts have been known that secreted various soluble factors, such as vascular endothelial growth factor (VEGF), transforming growth factor (TGF)-β, and insulin-like growth factor (IGF)-1 [13–15]. However, yet there is little understanding for the specific effect of hypoxia-inducible factor (HIF)-1α in osteoblasts under hypoxic environment in OA. A report on VEGF gene transcription in human osteoblast-like cells (MG63 cell lines) through the HIF-2α was demonstrated [16]. However, we consider that primary osteoblasts from human OA are more able to reflect the cellular phenotype after mechanical changes and HIF-1α is also one of target gene of T3 [17]. Therefore, it is extremely necessary to investigate the effect of HIF-1α in osteoblasts and angiogenesis in our study at least. In particular, elevated expression of these growth factors contributes to vascularization originating from subchondral bone and transits the tidemark to cartilage surface [18].

Previous study has reported that the increase of intracellular bioavailability of T3 was considered to influence OA onset, and the mechanism was unknown [19]. Activities of thyroid hormones are mainly mediated by THRs encoded by the THRA and THRB genes and regulate many organs' growth and mature, especially the process of skeletal development and remodeling [20]. Interestingly, VEGF, IGFs and placental growth factor (PGF) were target genes of THR signaling and play key roles in angiogenesis [21,22]. In addition, Moretto FC et al. [23] also confirmed that the upregulation of HIF-1α mRNA expression in response to T3 stimulation and it also participated in angiogenic activity. Hence, the purpose of present study was to explore whether locally elevated T3 bio-availability facilitated OA progression through abnormal THR signaling in OA osteoblasts. And our findings indicated that THRα signaling mainly regulated the expression of angiogenesis-related factors in OA osteoblasts, and THRα knockdown repressed angiogenic activities in subchondral bone, thereby attenuating OA development.

2. Materials and methods

2.1. Reagents

DMEM medium were purchased from Hyclone (Logan City, Utah, USA) and Fetal bovine serum (FBS) were purchased from CLARK (CLARK Bioscience, Australia). Anti-THRα, THRβ, HIF-1α, IGF-1 and anti-cluster designation 34 (CD34) antibodies were purchased from Abcam (Cambridge, UK). Anti-VEGF antibody was supplied from Elabscience Biotech Co., Ltd (Wuhan, China). ELISA kit was bought from Dakewe Biotech Co., Ltd (Dakewe Biotech, Shenzhen, China). Small interfering RNAs and 2′OMe + 5′Chol modified THRα siRNA labeled with 5Cy5 were supplied by Ribo Company. (RiboBio, Guangzhou, China). RNA reverse transcription and polymerase chain reaction system was bought from TaKaRa (TaKaRa Bio, Japan).

2.2. Human OA osteoblasts and chondrocytes culture

Knee tibial plateaus were harvested from patients with OA (12 females and 4 males, mean age 70.3 ± 7.9 years) undergoing total knee joint replacement and 5 healthy knee specimens (2 male, 3 females, mean age 66.8 ± 8.2 years) were obtained from amputees as normal control group. All patients have no diseases affecting bone metabolism and the history of hormone uses. Diagnose of knee osteoarthritis was based on American College of Rheumatology clinical criteria [24]. Demographic parameters were listed in Table 1. This study design was approved by the Ethical Committees of the first affiliated hospital of Anhui medical university and was carried out in accordance with the Helsinki Declaration.

According Kellgren-Lawrence (KL) grade [25], all bone samples were defined as KL grade III ~ IV OA. The subchondral bone plate samples of medial sclerosis zone were isolated after eliminating the trabecular bone, and were cut into small pieces of approximately 1–2 mm^2. The 1 mg/ml type I collagenase (Sigma, St. Louis, MO) in DMEM/F12 medium without serum was used to digest these bone chips at 37 °C for 20, 20, and 240 min sequentially. For chondrocytes culture, briefly, cartilage pieces were washed and digested in 0.5 mg/ml collagenase II solution with DMEM containing 2 mM L-glutamine, 50 U/ml penicillin G in 37 °C for 12–16 h. After centrifugation at 1000 rpm for 10 min, supernatant was seeded in DMEM medium containing 10% FBS at 37 °C incubator with a volume fraction of 5% CO_2 [26].

Table 1
Demographic parameters of OA patients and healthy controls.

	Age	Gender	K-L grade
Healthy controls	62	Male	0
	60	Female	0
	61	Female	0
	73	Male	0
	78	Female	0
OA	62	Male	IV
	60	Female	IV
	69	Female	IV
	72	Female	IV
	79	Male	III
	81	Male	IV
	63	Female	IV
	83	Female	III
	74	Female	III
	71	Male	IV
	69	Female	IV
	61	Female	IV

2.3. Mice

Twelve-week-old male C57BL/6 mice were purchased from Vital River Laboratory Animal Technology Co., Ltd. (Beijing, China). Mice subjected to a 12 h light/dark cycle and a standard food diet in the absence of specific pathogens. Mice were anesthetized and conducted the destabilization of the medial meniscus (DMM) on the left knee to induce surgical OA model. Sham surgeries were operated on independent mice. Healthy mice without any treatment served as the control group (n = 3–6 per group). All mice were killed at 8 weeks after surgery for immunohistochemistry. Additionally, to verify the effectiveness of the siRNA, mice were randomly divided into four groups: Sham, OA, OA + siControl, OA + THRα siRNA. From 4 weeks after surgery, mice were treated with intra-articular injection of 2 nmol 2′OMe + 5′Chol modified THRα siRNA labeled with 5Cy5 (OA + THRα siRNA group), scramble siRNA (OA + siControl group) at a weight ratio of 2 twice a week. A bioluminescence imaging (IVIS Lumia LTSeries III, PerkinElmer, USA) was used to verified that siRNA was injected into the knee joint cavity. All mice were euthanized at 8 weeks after injection. Animal experiments were approved and implemented by the Institutional Animal Care and Use Committee of the Anhui Medical University.

2.4. Measurement of human serum thyroid hormones

Blood samples from sixteen OA patients and sixteen age-matched healthy participants were collected to measure serum thyroid hormones, including TT3 (total triiodothyronine) and TT4 (total thyroxine). All blood samples were taken after a 12 h of fasting overnight. According to manufacturer's instruction, Cobas 601 fully automatic chemiluminescence analyzer (Roche, Basel, Switzerland) was used to measure these blood indicators.

2.5. Histochemistry, immunohistochemistry and immunofluorescence staining.

The well-prepared subchondral bone specimens of human and mice were soaked with 4% paraformaldehyde, decalcified with 10%

Table 2
Sequences of gene-specific primers and mRNA probes.

Genes	Primers sequence		Length (bp)
	Forward	Reverse	
THRA	AGGTCACCAGATGGAAAGCG	AGTGATAACCAGTTGCCTTGTC	110
THRB	TGGGACAAACCGAAGCACTG	TGGCTCTTCCTATGTAGGCAG	247
VEGF	AGGGCAGAATCATCACGAAGT	AGGGTCTCGATTGGATGGCA	202
HIF-1α	TGATTGCATCTCCATCTCCTACC	GACTCAAAGCGACAGATAACACG	177
IGF-1	TCAGCAGTCTTCCAACCCAAT	CATACCCTGTGGGCTTGTTG	228
ADAMTS5	GAGCCTGGAAGTGAGCAAGAA	CACATAAATCCTCCCGAGTAAACA	137
MMP13	ACTGAGAGGCTCCGAGAAATG	GAACCCCGCATCTTGGCTT	103
MMP9	GCACGACGTCTTCCAGTACC	GGTTCAACTCACTCCGGGAA	86
Actin	CACCCAGCACAATGAAGATCAAGAT	CCAGTTTTTAAATCCTGAGTCAAGC	317
THRα probe	5′-DIG-GUGUUUGCGGUGGUUGACGUAGUGC-DIG-3′		
THRβ probe	5′-DIG-CAGUGGCUGCCUUGGGCGUUGGUC-DIG-3′		

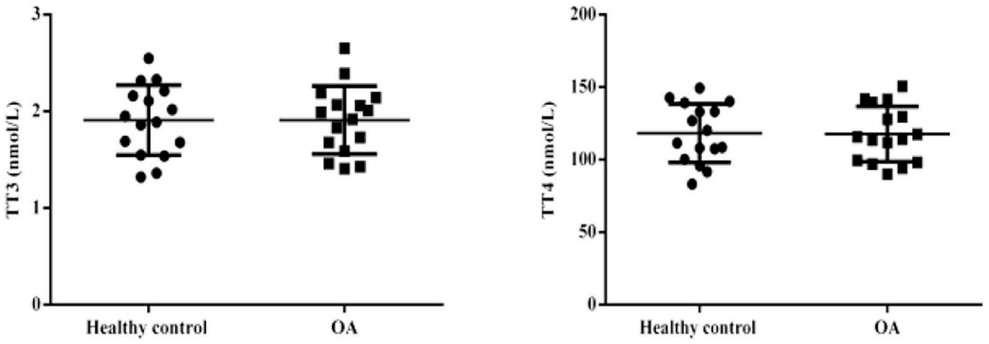

Fig. 1. Comparison of the TT3 and TT4 levels in serum between healthy control group and OA group.

ethylenediaminetetraacetid acid (EDTA) and embedded in paraffin. Sections (5 μm) were processed for hematoxylin-eosin (H&E) and safranin O and fast green staining using a manufacturer's protocol. Then, these slices were dewaxed in xylene for three times with 5 min each and subsequently rehydrated in gradient concentrations of ethanol. Samples were incubated in sodium citrate solution buffer at 92 °C for 10 min. In order to deactivate endogenous peroxidase, 0.3% H_2O_2 was dropwise added in tissue sections to block. Then, slices were incubated with anti-THRα (1:200 dilution; ab53729, Abcam), anti-THRβ (1:200 dilution; ab5622, Abcam), anti-CD34 (1:2500 dilution; ab81289, Abcam) for subchondral bone of human specimens and anti-MMP13 (1:100 dilution; E-AB-70346, Elabscience) and anti-MMP9 (1:200 dilution; 10375-2- AP, proteintech) for cartilage of mice at 4 °C overnight, followed by staining with goat anti-rabbit second antibodies conjugated with HRP next day. Each immunostained section was imaged with a light microscope and analysis results were shown using image J software. For immunofluorescence staining, OA osteoblasts were fixed in 4% buffered paraformaldehyde and then were incubated with specific antibody after penetrating cell membrane using 0.5% Triton X-100 and second antibody conjugated with fluorescence for 1 h at room temperature. The staining images were captured by confocal laser scanning microscopy (LSM880, Carl Zeiss Co.,Ltd, Germany).

2.6. Western blotting and ELISA

Osteoblasts lysates were extracted by nuclear and cytoplasmic extraction reagents kit (KeyGen Bio TECH, Nanjing, China). The concentrations of proteins were determined using bicinchoninic acid protein assay. The 15 μg protein from each sample was added to polyacrylamide gels and separated by 10% SDS-PAGE based on standard electrophoresis conditions. Proteins were transferred to PVDF membranes (Millipore, USA) and blocked in 5% skim milk. After incubation in primary antibodies, including anti-THRα (1:1000 dilution; ab53729, Abcam), anti-THRβ (1:1000 dilution; ab5622, Abcam), anti-VEGF at 1:1000 dilution (E-AB-64131, Elabscience), anti–HIF–1α (1:1000 dilution; ab51608, Abcam), anti-IGF-1 (1:1000 dilution; ab9572, Abcam), anti-GAPDH at 1:1000 dilution (GB11002, Servicebio, Wuhan) and anti-Histone H3 (1:1000 dilution; ab1791, Abcam) for osteoblasts and anti-MMP13 at 1:1000 dilution (E-AB-70346, Elabscience), anti-MMP9 (1:1000 dilution; 10375-2-AP, proteintech) for chondrocytes, membranes were incubated with goat anti-rabbit antibody and used an enhanced chemiluminescence kit to visualized these protein bands by Bio-Rad XRS + imaging system. The proteins intensity was assessed by image J software. Meanwhile, we detected the secretion levels of VEGF in the cell supernatant using the ELISA kit following the manufacturer's instructions.

2.7. Total RNA extraction and RT-qPCR

Total RNA from osteoblasts was extracted using TRIzol lysate (Invitrogen, USA) and reverse transcription was performed using a PrimeScript™RT reagent Kit according to manufactures' protocols after measurement of RNA concentration. Then, PCR reaction systems were: 95 °C for 5 min; followed by 40 cycles of: 95 °C for 30 s, 60 °C for 30 s, 72 °C for 1 min; followed by 72 °C for 10 min. Ct (cycle threshold) values were calculated using $2^{-\Delta\Delta CT}$ method to quantify relative genes expression. Sequences of gene-specific primers were shown in Table 2.

2.8. Small interfering RNAs (siRNAs) and cell transfection

OA osteoblasts were seeded at a density of 1×10^5 cells/well in 6-well plate and transfected with small interfering RNAs (Ribio, Guangzhou, china) to knockdown endogenous THRα and THRβ expression for 48 h. The target sequences of siRNAs for human were as follows: 5′-CTACCGCTGTATCACTTGT -3′ for THRα and 5′-GAACGACCAGAGTG TCTCA-3′ for THRβ. Fluorescence microscope IX51 (Olympus, Tokyo, Japan) and RT-qPCR were employed to detected the transfection efficiency. Osteoblasts transfected with siRNAs were cultured in DMEM/F12

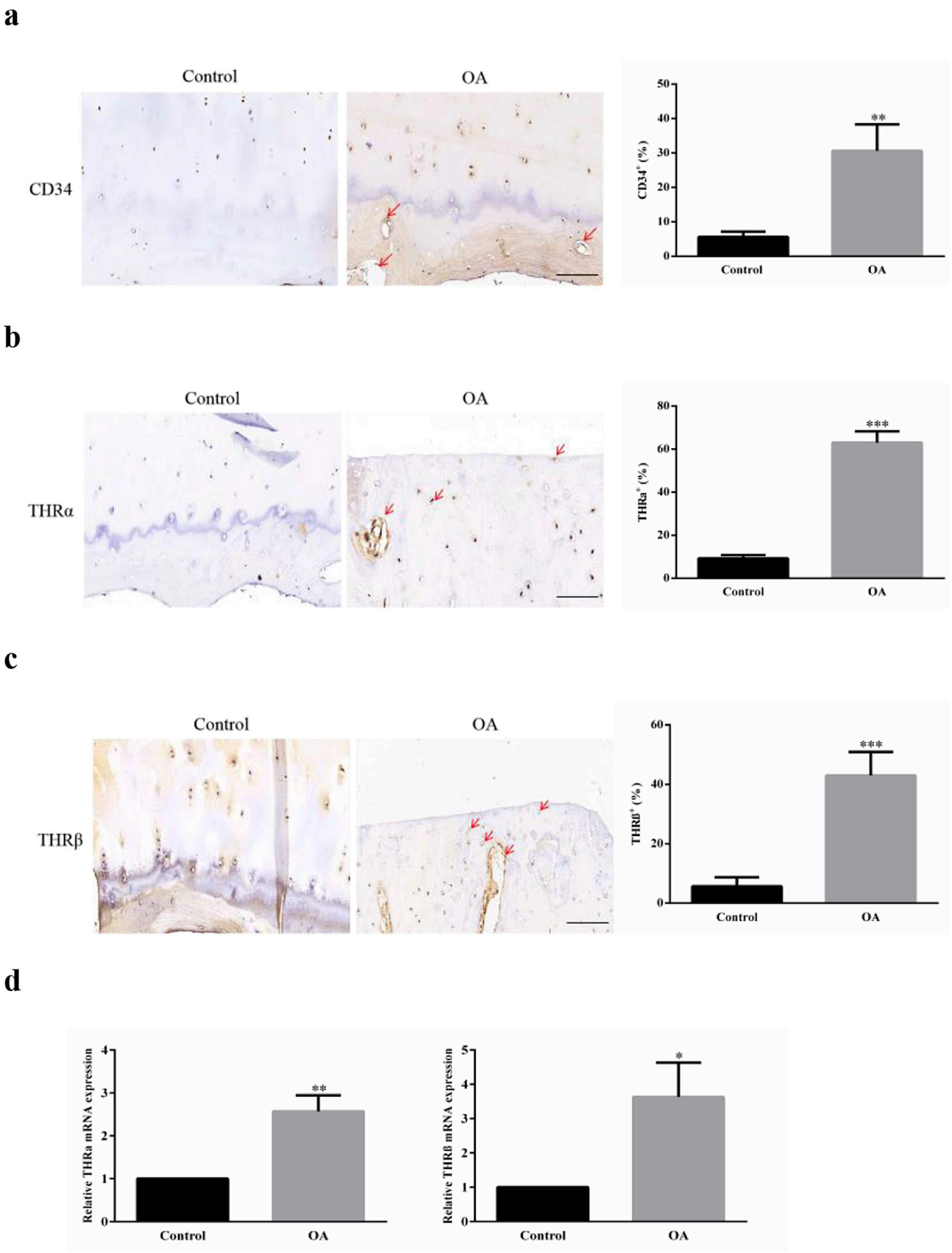

Fig. 2. The upregulation of THRα and THRβ expression in OA osteoblasts. **(a, b, c)** The CD34, THRα and THRβ staining of subchondral bone in OA group and healthy control group. Scale bar, 100 μm. Quantitative analysis of the number of positive cells was shown on the right. **(d)** The mRNA expression levels of THRα and THRβ in OA osteoblasts and healthy control osteoblats. **(e, f)** THRs expression levels from nuclear protein and total protein and quantitation of western blotting in osteoblasts. **(g)** Immunofluorescence detection of THRα and THRβ in osteoblasts. The yellow arrows indicate the enhancement of nuclear translocation of THRs in OA osteoblasts. Scale bar, 50 μm. Values are presented as the means ± SD. $^{*}P < 0.05$, $^{**}P < 0.01$ and $^{***}P < 0.001$ compared to the control group. (For interpretation of the references to colour in this figure legend, the reader is referred to the Web version of this article.)

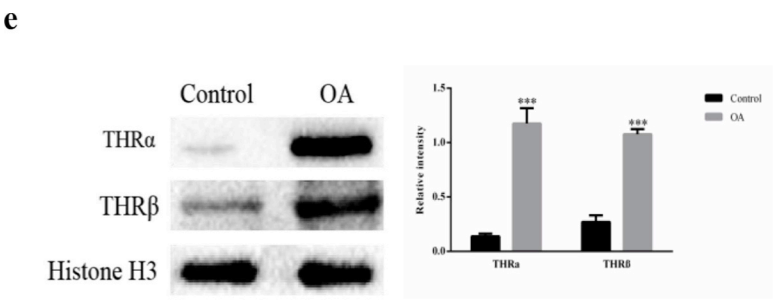

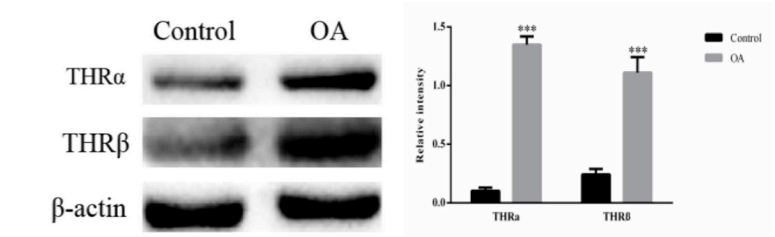

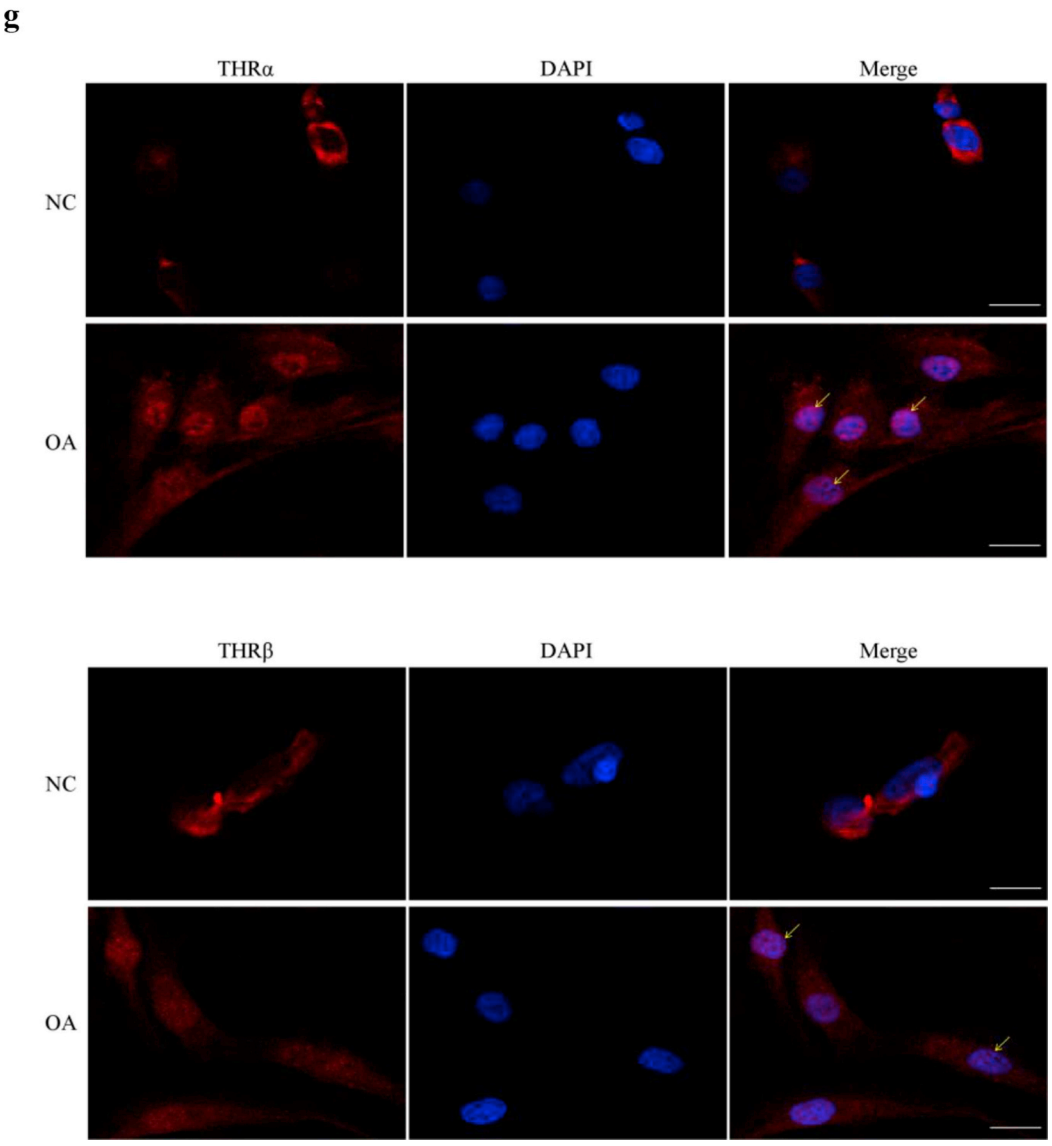

Fig. 2. (*continued*)

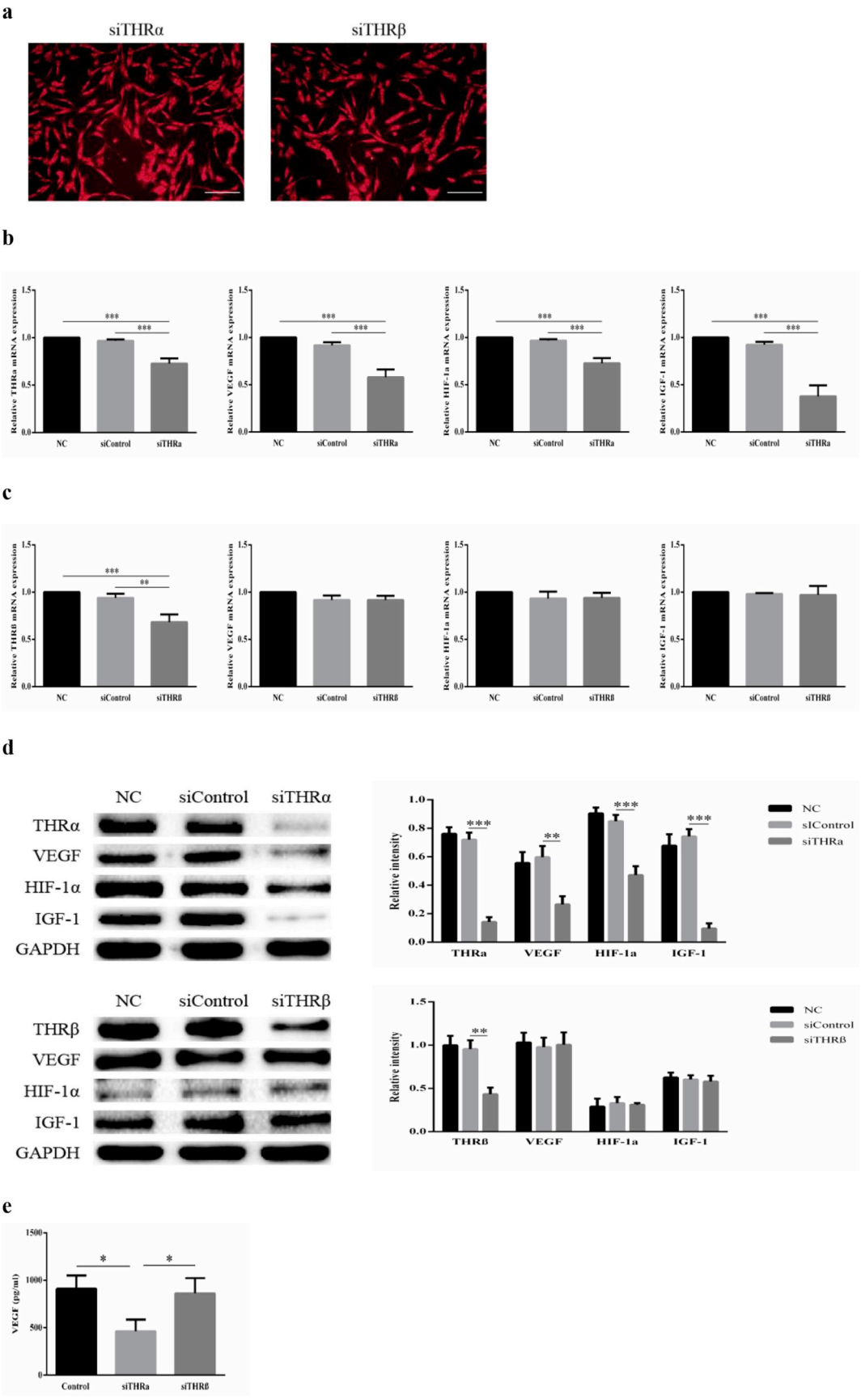

Fig. 3. The decreased expression of angiogenesis-related factors after THRα knockdown. **(a)** Red regions under fluorescent microscope show the transfection efficiency of small interfering RNA of THRα andTHRβ. Scale bar, 100 μm. **(b, c)** The mRNA expression levels of VEGF, HIF-1α and IGF-1 after THRs knockdown. **(d)** The protein expression levels of VEGF, HIF-1α and IGF-1 and quantification in osteoblasts after THRs knockdown. **(e)** Quantitative analysis of VEGF secretion levels in osteoblasts supernatant. Values are presented as the means ± SD. $^{*}P < 0.05$, $^{**}P < 0.01$ and $^{***}P < 0.001$. (For interpretation of the references to colour in this figure legend, the reader is referred to the Web version of this article.)

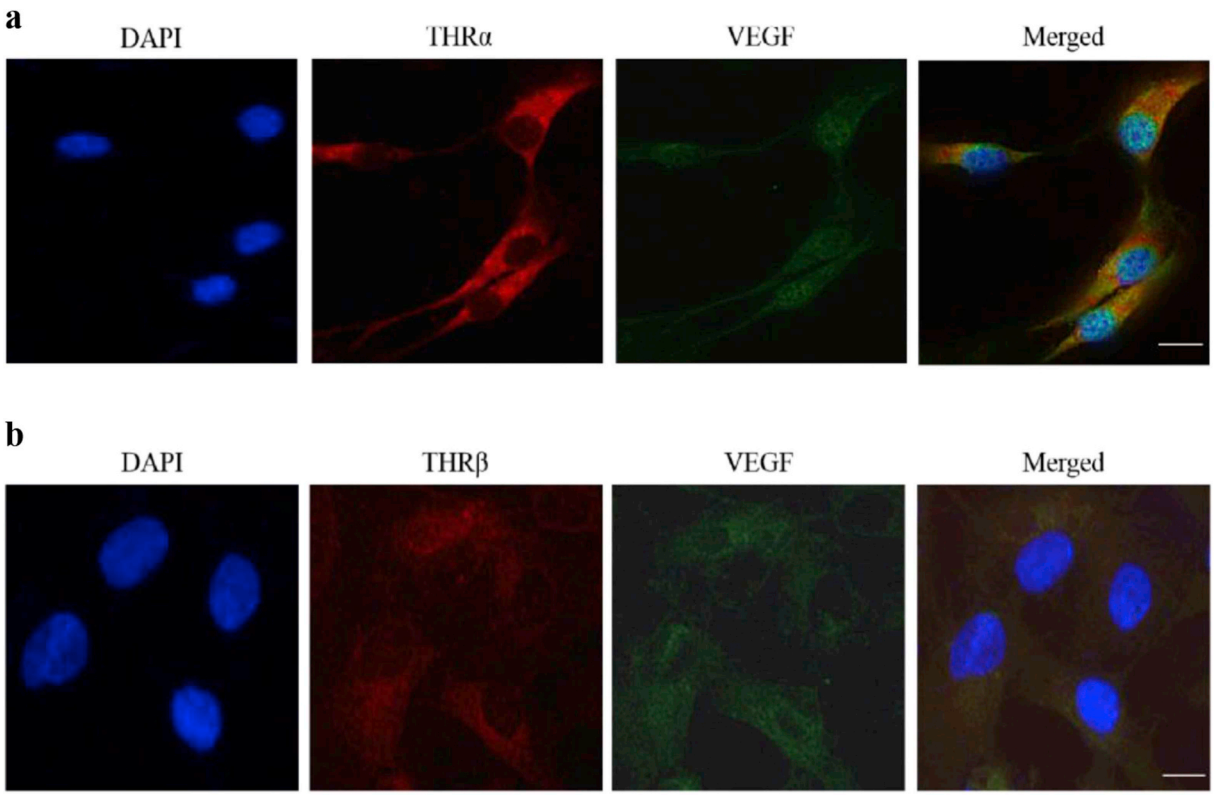

Fig. 4. THRα signaling mainly regulates the VEGF expression in OA osteoblasts. **(a, b)** The co-location of THRα and THRβ mRNA probes and VEGF in human OA osteoblasts by fluorescence in situ hybridization. Scale bar, 50 μm.

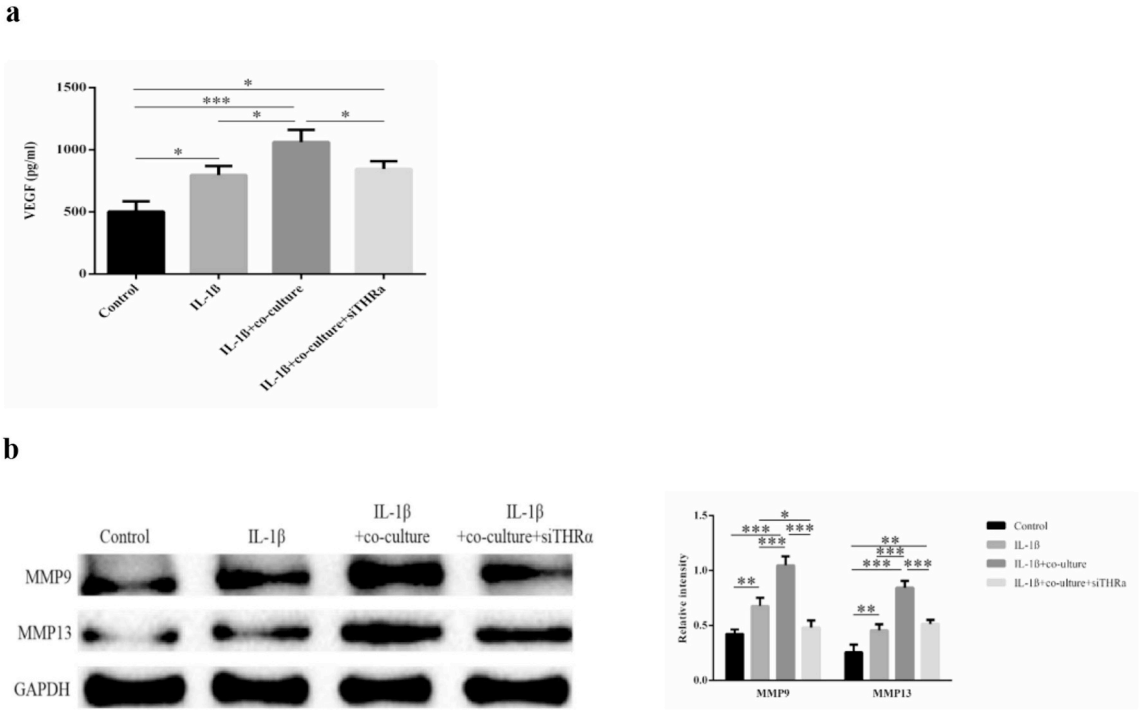

Fig. 5. MMPs expression of chondrocytes in co-culture model. **(a)** The secretion levels of VEGF in chondrocytes supernatant after different treatments. **(b)** The proteins expression levels of MMP9, MMP13 and quantification in OA chondrocytes after THRα knockdown of osteoblasts in 3D co-culture model. Values are presented as the means ± SD. $*P < 0.05$, $**P < 0.01$ and $***P < 0.001$.

medium without FBS and seeded into the Transwell chambers (Costar, Cambridge, MA). The chambers were inserted into the 6-well plates containing OA chondrocytes and 10% FBS to conduct 3D co-culture model for 48 h. The 10 ng/ml IL-1β stimulated chondrocytes to conduct OA model. The OA chondrocytes were divided into four groups: control group, IL-1β group, IL-1β + co-culture group and IL-1β + co-culture + siTHRα. ELISA and western blotting were used to examine the level of VEGF secretion and MMPs expression in chondrocytes.

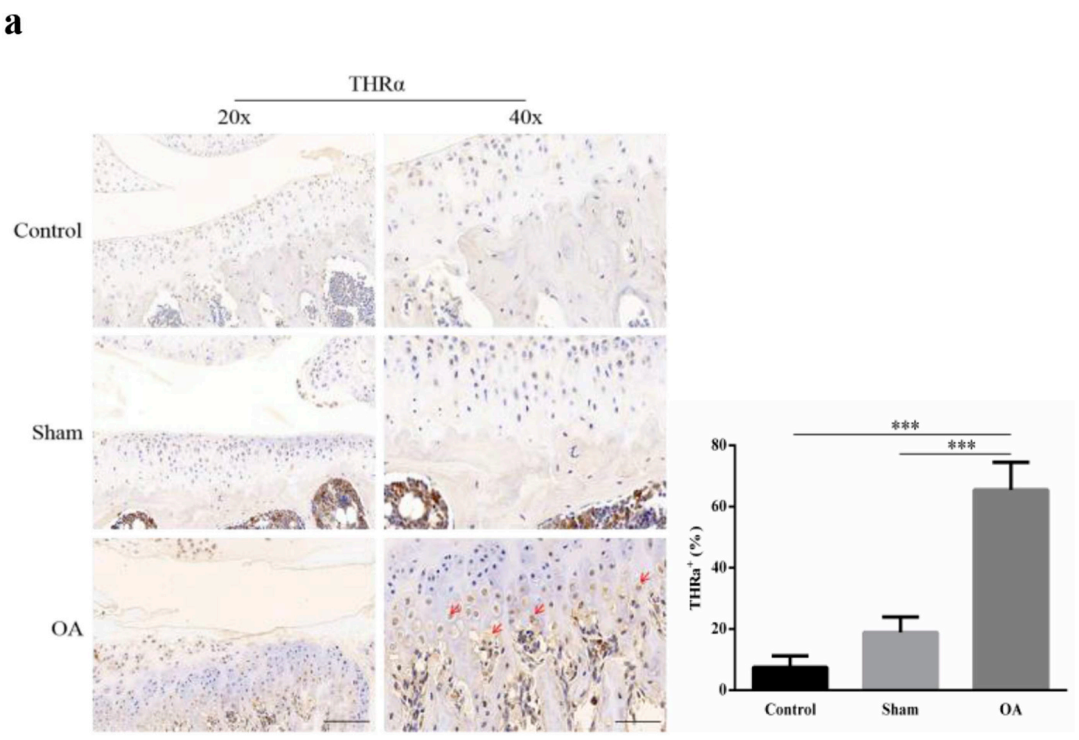

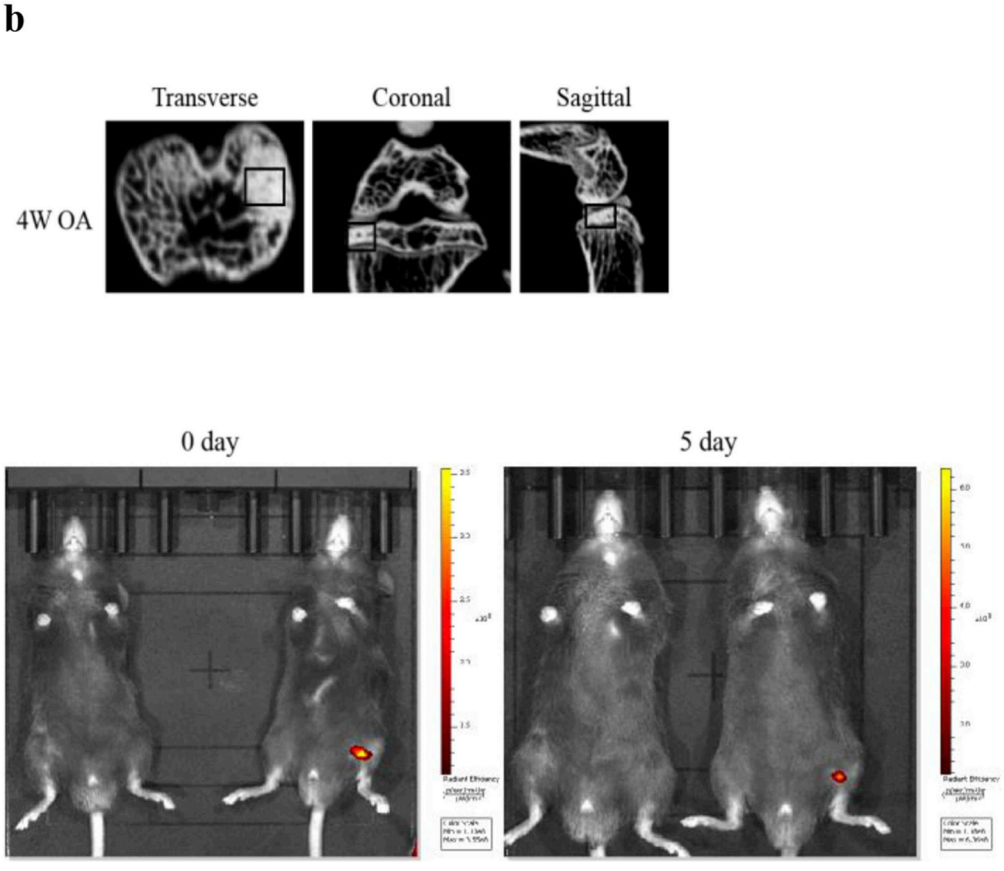

(caption on next page)

Fig. 6. Intra-articular injection with siTHRα reduces microangiogenic activities in subchondral bone and attenuates the cartilage degradation in OA model mice. **(a)** Immunohistochemistry and quantitative analysis of THRα (brown) in medial subchondral bone. Scale bars, left 100 μm, right 50 μm. Arrowheads represent THRα-positive cells. **(b)** Micro-CT showed the change of subchondral bone sclerosis at 4 weeks after DMM surgery and the results of bioluminescence imaging indicated that fluorescent emission was maintained at least 5 days after intra-articular injection with siTHRα. The black rectangles indicate sclerosis areas in subchondral bone. **(c)** H&E staining of the subchondral bone plate and cartilage. The thicknesses of hyaline cartilage (HC) and calcified cartilage (CC) were marked by double-headed arrows. CD34 and Safranin-O and fast green staining in Sham, OA, OA + sicontrol and OA + siTHRα groups. Scale bars, left 100 μm, right 50 μm. Arrowheads represent CD34-positive cells and quantitative analysis was showed on the right. **(d)** MMP13 and MMP9 staining in Sham, OA, OA + siControl and OA + siTHRα groups in medial articular cartilage. Scale bars, left 100 μm, right 50 μm. Arrowheads represent MMP13- and MMP9-positive cells and quantitative analysis was showed on the right. **(e)** Three dimensional microCT images of the medial compartment in tibial subchondral bone (sagittal view) in different groups were displayed and microstructural parameters of subchondral bone were analyzed. **(f)** OARSI scores in Sham, OA, OA + siControl and OA + siTHRα groups. Values are presented as the means ± SD. $^{*}P < 0.05$, $^{**}P < 0.01$; $^{***}P < 0.001$. (For interpretation of the references to colour in this figure legend, the reader is referred to the Web version of this article.)

2.9. mRNA fluorescence in situ hybridization (FISH)

The probes of THRα and THRβ mRNA were designed to confirm the main receptor associated with regulating VEGF expression. Following previous experimental instruction, primary human OA osteoblasts were seeded in an 6-well plate at a density of 1×10^5 cells/well and fixed in 4% paraformaldehyde, washed with PBS. Then, OA osteoblasts were incubated with 8 ng/μl THRα or THRβ mRNA probes at 37 °C overnight. As primary antibody, VEGF was added to slide at 1:200 dilution. Cell nucleus were stained with DAPI (4′,6-diamidino-2-phenylindole) after incubation of secondary antibody labeled FITC. Images were acquired using a fluorescence microscope.

2.10. Micro-CT

Left knee joints of mice removed soft tissue were dissected, fixed them in 98% ethanol for 24 h and visualized them by high-resolution in-vivo X-ray microtomograph (Skyscan1176, Bruker, Germany). A voltage 58 kVp, a current of 431 μA and a resolution of 9.0 μm per pixel were set in scanner. Images of three-dimensional reconstruction in subchondral bone medial compartment and parameters of the trabecular bone were obtained by the NRecon software. Additionally, these parameters of BMD (bone mineral density) and BV/TV (bone volume/total tissue volume) were analyzed.

2.11. Statistical analysis

All data are presented as the mean ± standard deviation (SD). Comparisons of different groups were performed by a one-way analysis of variance (ANOVA) SPSS V.23.0 (SPSS Inc., Chicago, USA) to assess statistical differences and the critical value was $P < 0.05$.

3. Results

3.1. The high expression and increased nuclear translocation of THRs in OA osteoblasts and unchanged serum levels of thyroid hormones in patients

We firstly measured the TT3 and TT4 levels of serum in OA patients and healthy controls (n = 16 per group), however, there was no statistical difference between two groups (Fig. 1). Then, as the blood endothelial cell marker, CD34 was used to evaluate the angiogenic activities and an obvious increase was revealed in human subchondral bone (Fig. 2a). Due to abnormal proliferation of OA osteoblasts, we first detected THRs expression. As shown in Fig. 2b ~ f, strong staining of THRα and THRβ were shown in OA subchondral bone tissues compared to control group. Consistently, the mRNA and protein levels of THRα and THRβ were also significantly upregulated in OA osteoblasts and the nuclear translocation of THRα and THRβ were obviously elevated. Hence, these results indicated the increase in local bio-availability of T3 may be attributed to the abnormal THRs signaling.

3.2. Inhibition of THRα signaling downregulated the expression of angiogenesis-related proteins

THRα siRNA and THRβ siRNA were designed to verify whether abnormal THRs signaling was involved in angiogenesis in OA subchondral bone, and the transfection efficiency in osteoblasts was observed under fluorescence microscope (Fig. 3a). As expected, RT-qPCR and western blotting analysis demonstrated that the expression of VEGF, IGF-1 and HIF-1α were significantly downregulated when THRα was knocked down. However, there is no statistical difference for these proteins expression after THRβ knockdown at mRNA and protein levels (Fig. 3b–d). Quantitative analysis by ELISA also suggested that the secretion level of VEGF in osteoblasts supernatant was decreased after THRα siRNA treatment (Fig. 3e).

3.3. THRα was the leading receptor of regulating microangiogenesis in subchondral bone

To further definite the mainly regulative effect of THRα signaling for angiogenesis, the regulation of VEGF expression in OA osteoblasts was determined by fluorescence in situ hybridization using the marker THRα mRNA and THRβ mRNA probes and VEGF antibody. As shown in Fig. 4, the fluorescence intensity of VEGF with THRα is much stronger than the binding of VEGF to THRβ.

3.4. Inhibition of THRα in osteoblast downregulated the MMPs expression in OA chondrocytes

Changes of biological phenotypes in osteoblasts and chondrocytes accelerate the OA progression, which affect each other. Thus, we next examined the effect of osteoblasts with THRα siRNA treatment on OA chondrocytes. According to previous study, the *in vitro* 3D co-culture model allowed us to explore cell-cell interactions and we investigated the expression of cartilage degradation-related proteins of MMP9 and MMP13 by transwell assay. As presented in Fig. 5, THRα siRNA-mediated THRα knockdown in OA osteoblasts decreased the secretion level of VEGF and MMP9, MMP13 expression in OA chondrocytes by the co-culture model.

3.5. Inhibition of THRα signaling attenuated cartilage impairment and subchondral bone sclerosis in OA model mice

To verify our *in vitro* findings, C57/BL mice at 12 weeks of age were conducted the model of DMM on the left knee joints and pathological changes were observed after different treatments. The strong staining of THRα in OA model mice was found compared to control group and sham group 8 weeks after surgery (Fig. 6a). And the change on subchondral bone sclerosis in mice 4 weeks after DMM was found by micro-CT, suggesting that OA was in an period of aberrant bone formation dominated by proliferative osteoblasts. Due to non-homology of THRβ siRNA with human, THRα siRNA was only employed for intra-articular injection in OA model mice. The bioluminescence imaging was used to prove that the THRα siRNA labeled fluorescence injected into

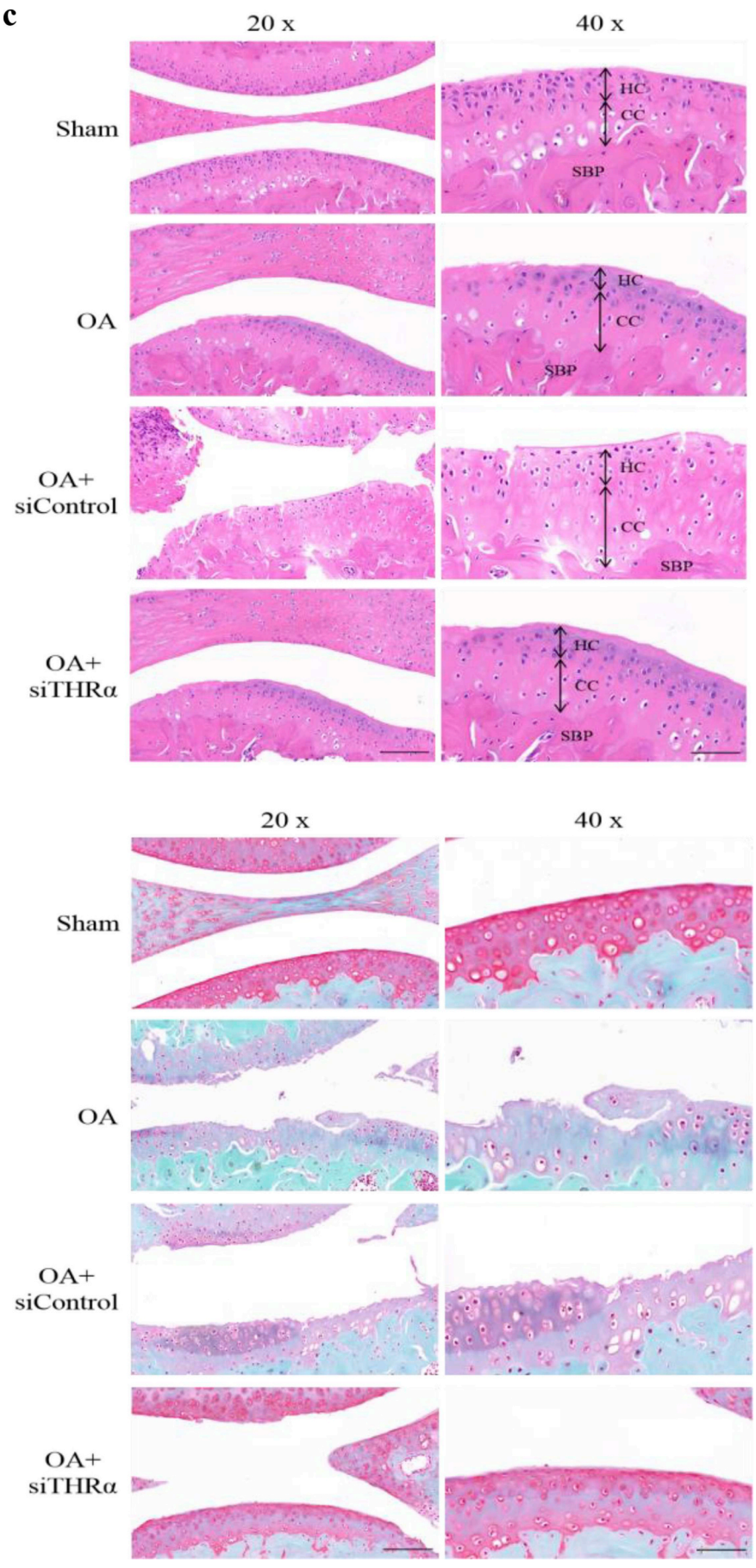

Fig. 6. (*continued*)

knee joints cavity and still detected the fluorescence after 5 days (Fig. 6b). Unexpectedly, H&E staining showed that the thickness of the calcified cartilage zone in those mice with THRα siRNA injection was lower than that of OA model mice without treatment. We also found that the number of CD34 positive cells was markedly reduced in subchondral bone and proteoglycan loss of articular cartilage were alleviated in THRα siRNA group by immunohistochemtry and Safranin-O and fast green staining (Fig. 6c and d). Additionally, the parameters of microarchitecture of subchondral bone, especially increased BMD and BV/TV in OA + siTHRα group revealed that aberrant subchondral bone formation was also ameliorated (Fig. 6e). Meanwhile, OARSI scoring of OA severity was used to assess the injury-degree of articular cartilage among four groups (Fig. 6f).

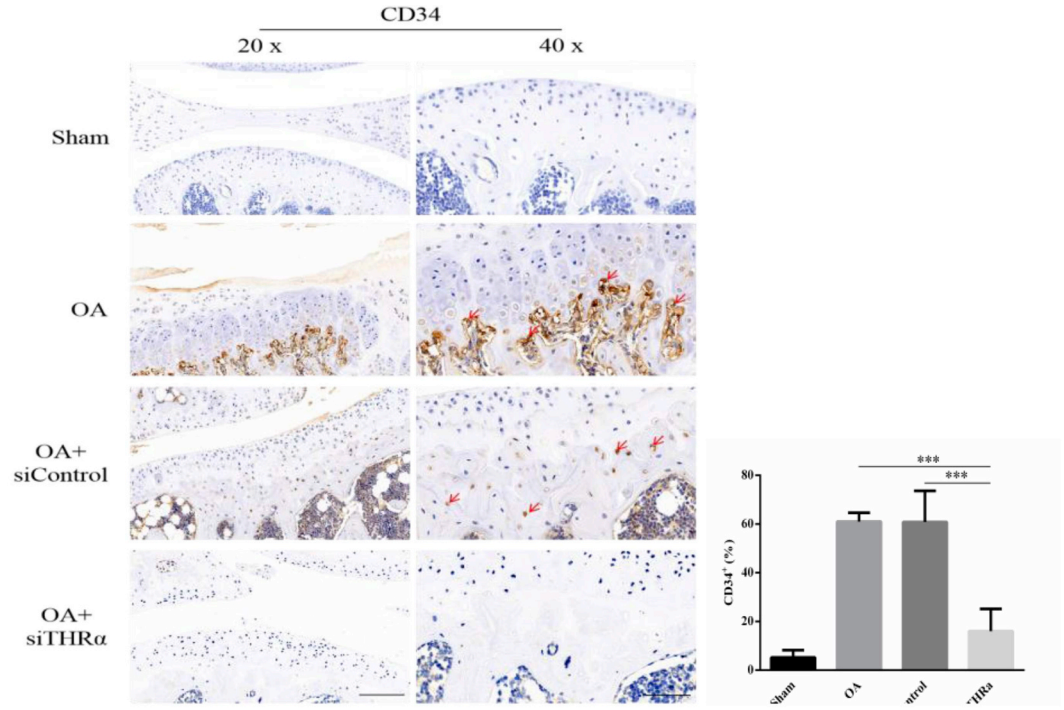

d

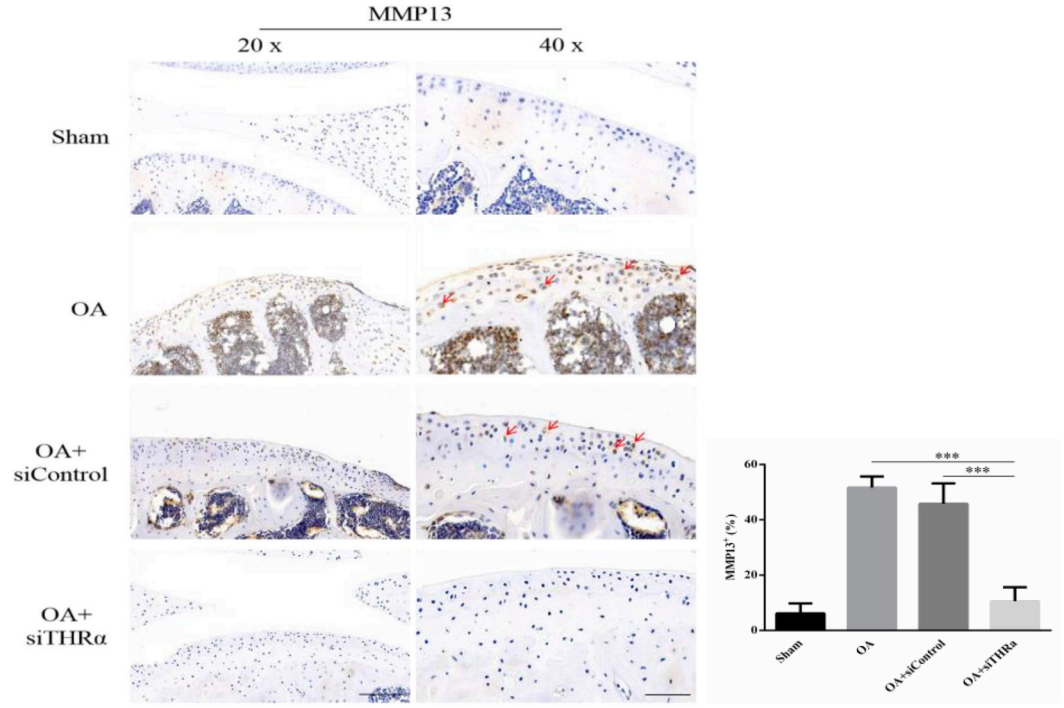

Fig. 6. (*continued*)

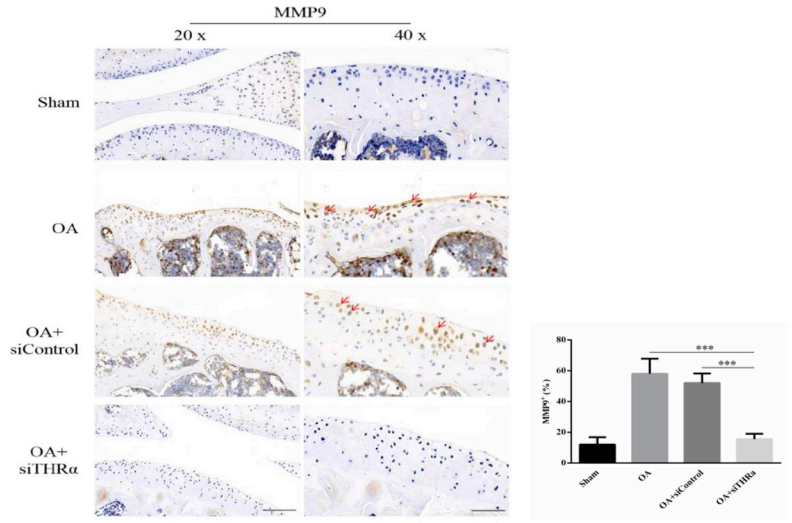

e

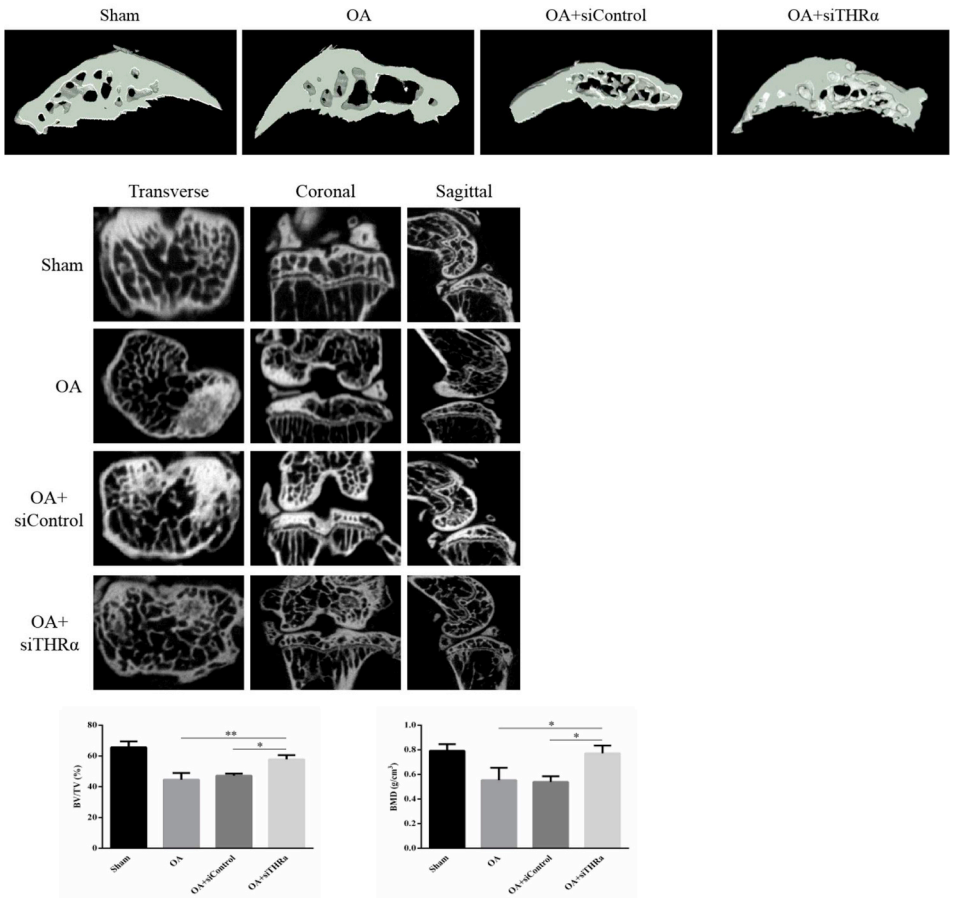

f

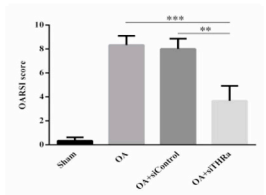

Fig. 6. (*continued*)

4. Discussion

Thyroid hormones are known for its biological effects combined with THRs on skeletal growth and metabolism, especially the regulation of bone homeostasis [27,28]. Linked to the abnormal proliferation of osteoblasts in OA [15] and the uncertain mechanism of locally elevated T3 bio-availability, we firstly found a significant increase of THRs expression in OA osteoblasts and subchondral bone compared to normal controls. Consistently, the stronger staining of THRα-positive was observed in OA model mice. In fact, a recent study from health toxicology have also reported that exposure of gestational Di-(2-ethylhexyl) phthalate lead to fetal intrauterine growth restriction, which may be attributed to local THR signaling disorders without effect on systemic thyroid hormone levels, suggesting that local T3 played a key role in mechanism of disease onset [29]. Hence, whether this locally disturbed THRs signaling enhanced T3 bio-availability and contributed to microangiogenesis in subchondral bone are critical points of interest in our study.

Relative to aberrant bone formation in OA, the coupled with microangiogenesis in subchondral bone is a crucial factor in cartilage degradation [30–32]. A variety of angiogenesis-related factors were considered to be the downstream proteins of the THR signaling. Our data indicated that the downregulation of VEGF, HIF-1α and IGF-1 expression in OA osteoblasts after inhibition of THRα signaling *in vitro*. Indeed, the decrease of positive cells number of CD34 in the subchondral bone of OA model mice further demonstrated the reduced angiogenic activities. The blockage of microangiogenesis could prevent the transport of MMPs and harmful small molecules from subchondral bone, which alleviated the degradation of OA articular cartilage. In our study, it was once again confirmed that the vascular invasion established the interaction in osteochondral unit for OA progression [33,34].

Recently, the function of THRs have been gradually clarified. Studies demonstrated that trabecular bone volume and mineralization were increased in mutant THRα mice and severe osteoporosis was displayed in mutant THRβ mice [35]. Surprisedly, as the most important factor in angiogenesis, the reduction of VEGF expression in osteoblasts after inhibition of THRβ in our study was much lower than that of THRa knockdown. Meanwhile, this result of fluorescence in situ hybridization further confirmed that abnormal THRα signaling of osteoblasts may act as a crucial role in regulating microangiogenesis in subchondral bone during OA progression. However, this may be inconsistent with the view that angiogenesis in pathological cardiac hypertrophy was regulated by THRβ signaling [36]. We believe that this was caused by the difference in cell phenotype and the biological environment in which these were located. And a recent study in breast cancer cell lines concluded that depletion of THRα did not influence cell proliferation or viability *in vitro* [37]. Thus, whether THRβ regulated the abnormal proliferation of OA osteoblasts requires further exploration.

Previous studies regarding the effect of VEGF in OA progression have provided evidences and VEGF plays a proactive role in inducing and activating MMP-1, MMP-3, MMP-9 and MMP-13 expression in chondrocytes [38,39]. These findings were consistent with these results of *in vitro* co-culture model in our study. As a consequence, THRα siRNA-mediated THRα downregulation decreased the VEGF secretion in osteoblasts and subsequently reduced MMPs expression in chondrocytes. Moreover, MMPs have also been reported that could facilitate VEGF release and thereby initiating the angiogenic activities [40]. Additionally, VEGF is not only involved in the cartilage degradation but also participated in the process of osteophyte formation in OA [41,42].

OA model mice elucidated the function of intra-articular injection with THRα siRNA *in vivo* study, as demonstrated by OARSI scores [43], which were showed to be distinctly decreased in the THRα siRNA group relative to time-matched OA group. Notely, THRα2 rather than THRα1regulated skeletal maturity and the THRα siRNA was used in our study referred to THRα1 [44]. Our data revealed that the angiogenic activities of subchondral bone were reduced in THRα siRNA group compared to the OA group by staining of vascular endothelial cell marker. These results of immunohistochemistry *in vivo* explained, at least partially, the regulative effect of abnormal THR signaling for angiogenesis in OA. Analogously, OA-like pathological changes, including cartilage loss, subchondral bone sclerosis, and osteophyte formation were induced in a report after local intra-articular injection with VEGF in the knee joints of mice [45]. Indeed, treatment targeting VEGF may be further valuable for the drugs research and development in OA [46]. Changes on decreased proteoglycans loss, weak staining of MMP9 and MMP13 in articular cartilage after THRα siRNA treatment in OA model mice revealed that THRα knockdown ameliorated cartilage degradation *in vivo*. Moreover, the increased BMD and BV/TV, and lower thickness of the calcified cartilage zone after THRα siRNA injection implied the attenuation of aberrant subchondral bone formation in OA model mice. Meanwhile, the most important limitation of the present study is that the number of healthy knee samples is too small. Also, this study cannot completely clarify the function of THRβ in OA osteoblasts. Moreover, the regulative mechanism of THRα for angiogenesis in OA animal model still needs further explore.

5. Conclusions

Our present findings demonstrate that abnormal THRα signaling of osteoblasts contributes to locally upregulated T3 bio-availability, and regulate microangiogenesis in subchondral bone. Therefore, inhibition of THRα signaling could be a novel potential approach for preventing OA progression.

Funding

This study was supported by the National Natural Science Foundation of China (No. 81672161).

Declaration of competing interest

All authors have no conflict of interest in this work.

Acknowledgment

Zongsheng Yin and Chen Zhu designed the study; Lei Li, Meng Li and Yiqun Pang performed this experiments. Lei Li, Jun Wang and Yunpeng Wan analyzed experimental data; Lei Li, Meng Li and Yiqun Pang wrote this manuscript.

Appendix A. Supplementary data

Supplementary data to this article can be found online at https://doi.org/10.1016/j.lfs.2019.116975.

References

[1] J.M. Hootman, C.G. Helmick, Projections of US prevalence of arthritis and associated activity limitations, Arthritis Rheum. 54 (2006) 226–229.
[2] Y. Henrotin, L. Pesesse, C. Sanchez, Subchondral bone and osteoarthritis: biological and cellular aspects, Osteoporos. Int. 23 (Suppl 8) (2012) S847–S851.
[3] E. Abed, D. Couchourel, A. Delalandre, N. Duval, J.P. Pelletier, J. Martel-Pelletier, et al., Low sirtuin 1 levels in human osteoarthritis subchondral osteoblasts lead to abnormal sclerostin expression which decreases Wnt/beta-catenin activity, Bone 59 (2014) 28–36.
[4] J.L. Hamilton, M. Nagao, B.R. Levine, D. Chen, B.R. Olsen, H.J. Im, Targeting VEGF and its receptors for the treatment of osteoarthritis and associated pain, J. Bone Miner. Res. 31 (2016) 911–924.
[5] T. Funck-Brentano, M. Cohen-Solal, Crosstalk between cartilage and bone: when bone cytokines matter, Cytokine Growth Factor Rev. 22 (2011) 91–97.
[6] M. Zarka, E. Hay, A. Ostertag, C. Marty, C. Chappard, F. Oudet, et al., Microcracks in subchondral bone plate is linked to less cartilage damage, Bone 123 (2019) 1–7.
[7] M.R. Klement, P.F. Sharkey, The significance of osteoarthritis-associated bone marrow lesions in the knee, J. Am. Acad. Orthop. Surg. (2019), https://doi.org/10.5435/JAAOS-D-18-00267.

[8] M. Mahjoub, F. Berenbaum, X. Houard, Why subchondral bone in osteoarthritis? The importance of the cartilage bone interface in osteoarthritis, Osteoporos. Int. 23 (Suppl 8) (2012) S841–S846.
[9] H. Madry, C.N. van Dijk, M. Mueller-Gerbl, The basic science of the subchondral bone, Knee Surg. Sport. Traumatol. Arthrosc. 18 (2010) 419–433.
[10] I. Prasadam, S. van Gennip, T. Friis, W. Shi, R. Crawford, Y. Xiao, ERK-1/2 and p38 in the regulation of hypertrophic changes of normal articular cartilage chondrocytes induced by osteoarthritic subchondral osteoblasts, Arthritis Rheum. 62 (2010) 1349–1360.
[11] B. Huang, W. Wang, Q. Li, Z. Wang, B. Yan, Z. Zhang, et al., Osteoblasts secrete Cxcl9 to regulate angiogenesis in bone, Nat. Commun. 7 (2016) 13885.
[12] N. Maruotti, A. Corrado, F.P. Cantatore, Osteoblast role in osteoarthritis pathogenesis, J. Cell. Physiol. 232 (2017) 2957–2963.
[13] A. Corrado, A. Neve, F.P. Cantatore, Expression of vascular endothelial growth factor in normal, osteoarthritic and osteoporotic osteoblasts, Clin. Exp. Med. 13 (2013) 81–84.
[14] D.D. Kumarasinghe, T. Sullivan, J.S. Kuliwaba, N.L. Fazzalari, G.J. Atkins, Evidence for the dysregulated expression of TWIST1, TGFbeta1 and SMAD3 in differentiating osteoblasts from primary hip osteoarthritis patients, Osteoarthr. Cartil. 20 (2012) 1357–1366.
[15] Frédéric Massicotte, Isabelle Aubry, Johanne Martel-Pelletier, Jean-Pierre Pelletier, Julio Fernandes, Daniel Lajeunesse, Abnormal insulin-like growth factor 1 signaling in human osteoarthritic subchondral bone osteoblasts, Arthritis Res. Ther. 8 (2006) R177.
[16] N. Akeno, M.F. Czyzyk-Krzeska, T.S. Gross, T.L. Clemens, Hypoxia induces vascular endothelial growth factor gene transcription in human osteoblast-like cells through the hypoxia-inducible factor-2alpha, Endocrinology 142 (2001) 959–962.
[17] Lars C. Moeller, Alexandra M. Dumitrescu, Robert L. Walker, et al., Thyroid hormone responsive genes in cultured human fibroblast, J. Clin. Endocrinol. Metab. 90 (2005) 936–943.
[18] S.M. Chim, J. Tickner, S.T. Chow, V. Kuek, B. Guo, G. Zhang, et al., Angiogenic factors in bone local environment, Cytokine Growth Factor, Rev. 24 (2013) 297–310.
[19] I. Meulenbelt, S.D. Bos, K. Chapman, R. van der Breggen, J.J. Houwing-Duistermaat, D. Kremer, et al., Meta-analyses of genes modulating intracellular T3 bio-availability reveal a possible role for the DIO3 gene in osteoarthritis susceptibility, Ann. Rheum. Dis. 70 (2011) 164–167.
[20] J.A. Waung, J.H. Bassett, G.R. Williams, Thyroid hormone metabolism in skeletal development and adult bone maintenance, Trends Endocrinol. Metab. 23 (2012) 155–162.
[21] W. Xing, K.E. Govoni, L.R. Donahue, C. Kesavan, J. Wergedal, C. Long, et al., Genetic evidence that thyroid hormone is indispensable for prepubertal insulin-like growth factor-I expression and bone acquisition in mice, J. Bone Miner. Res. 27 (2012) 1067–1079.
[22] M.K. Luidens, S.A. Mousa, F.B. Davis, H.Y. Lin, P.J. Davis, Thyroid hormone and angiogenesis, Vasc. Pharmacol. 52 (2010) 142–145.
[23] F.C. Moretto, M.T. De Sibio, A.C. Luvizon, R.M. Olimpio, M. de Oliveira, C.A. Alves, et al., Triiodothyronine (T3) induces HIF1A and TGFA expression in MCF7 cells by activating PI3K, Life Sci. 154 (2016) 52–57.
[24] R.D. Altman, Criteria for classification of clinical osteoarthritis, J. Rheumatol. Suppl. 27 (1991) 10–12.
[25] J.H. Kellgren, J.S. Lawrence, Radiological assessment of osteoarthrosis, Ann. Rheum. Dis. 16 (1957) 494–502.
[26] A.W. Cheng, T.V. Stabler, M. Bolognesi, V.B. Kraus, Selenomethionine inhibits IL-1beta inducible nitric oxide synthase (iNOS) and cyclooxygenase 2 (COX2) expression in primary human chondrocytes, Osteoarthr. Cartil. 19 (2011) 118–125.
[27] G.R. Williams, Thyroid hormone actions in cartilage and bone, Eur Thyroid J 2 (2013) 3–13.
[28] E. Tsourdi, J. Colditz, F. Lademann, E. Rijntjes, J. Kohrle, C. Niehrs, et al., The role of dickkopf-1 in thyroid hormone-induced changes of bone remodeling in male mice, Endocrinology 160 (2019) 664–674.
[29] Z. Yu, Y. Han, R. Shen, K. Huang, Y.Y. Xu, Q.N. Wang, et al., Gestational di-(2-ethylhexyl) phthalate exposure causes fetal intrauterine growth restriction through disturbing placental thyroid hormone receptor signaling, Toxicol. Lett. 294 (2018) 1–10.
[30] Z. Ma, X. Jin, Z. Qian, F. Li, M. Xu, Y. Zhang, et al., Deletion of clock gene Bmal1 impaired the chondrocyte function due to disruption of the HIF1alpha-VEGF signaling pathway, Cell Cycle 18 (2019) 1473–1489.
[31] L. Pesesse, C. Sanchez, Y. Henrotin, Osteochondral plate angiogenesis: a new treatment target in osteoarthritis, Jt. Bone Spine 78 (2011) 144–149.
[32] D.A. Walsh, D.F. McWilliams, M.J. Turley, M.R. Dixon, R.E. Fransès, P.I. Mapp, et al., Angiogenesis and nerve growth factor at the osteochondral junction in rheumatoid arthritis and osteoarthritis, Rheumatology 49 (2010) 1852–1861.
[33] X.L. Yuan, H.Y. Meng, Y.C. Wang, J. Peng, Q.Y. Guo, A.Y. Wang, et al., Bone-cartilage interface crosstalk in osteoarthritis: potential pathways and future therapeutic strategies, Osteoarthr. Cartil. 22 (2014) 1077–1089.
[34] J. Lu, H. Zhang, D. Cai, C. Zeng, P. Lai, Y. Shao, et al., Positive-feedback regulation of subchondral H-type vessel formation by chondrocyte promotes osteoarthritis development in mice, J. Bone Miner. Res. 33 (2018) 909–920.
[35] J.H. Bassett, G.R. Williams, The skeletal phenotypes of TRalpha and TRbeta mutant mice, J. Mol. Endocrinol. 42 (2009) 269–282.
[36] A. Makino, J. Suarez, H. Wang, D.D. Belke, B.T. Scott, W.H. Dillmann, Thyroid hormone receptor-beta is associated with coronary angiogenesis during pathological cardiac hypertrophy, Endocrinology 150 (2009) 2008–2015.
[37] M.J. Elliott, K.J. Jerzak, J.G. Cockburn, Z. Safikhani, W.D. Gwynne, J.A. Hassell, et al., The antiarrhythmic drug, dronedarone, demonstrates cytotoxic effects in breast cancer independent of thyroid hormone receptor alpha 1 (THRalpha1) antagonism, Sci. Rep. 8 (2018) 16562.
[38] T. Pufe, V. Harde, W. Petersen, M.B. Goldring, B. Tillmann, R. Mentlein, Vascular endothelial growth factor (VEGF) induces matrix metalloproteinase expression in immortalized chondrocytes, J. Pathol. 202 (2004) 367–374.
[39] J. Zupan, P. Vrtacnik, A. Cor, G. Haring, G. Weryha, S. Visvikis-Siest, et al., VEGF-A is associated with early degenerative changes in cartilage and subchondral bone, Growth Factors 36 (2018) 263–273.
[40] A.M. Mahecha, H. Wang, The influence of vascular endothelial growth factor-A and matrix metalloproteinase-2 and -9 in angiogenesis, metastasis, and prognosis of endometrial cancer, OncoTargets Ther. 10 (2017) 4617–4624.
[41] K. Murata, T. Kokubun, Y. Morishita, K. Onitsuka, S. Fujiwara, A. Nakajima, et al., Controlling abnormal joint movement inhibits response of Osteophyte Formation, Cartilage 9 (2018) 391–401.
[42] S. Wang, C. Zhou, H. Zheng, Z. Zhang, Y. Mei, J.A. Martin, Chondrogenic progenitor cells promote vascular endothelial growth factor expression through stromal-derived factor-1, Osteoarthr. Cartil. 25 (2017) 742–749.
[43] K.P. Pritzker, S. Gay, S.A. Jimenez, K. Ostergaard, J.P. Pelletier, P.A. Revell, et al., Osteoarthritis cartilage histopathology: grading and staging, Osteoarthr. Cartil. 14 (2006) 13–29.
[44] J.H. Bassett, P.J. O'Shea, S. Sriskantharajah, B. Rabier, A. Boyde, P.G. Howell, et al., Thyroid hormone excess rather than thyrotropin deficiency induces osteoporosis in hyperthyroidism, Mol. Endocrinol. 21 (2007) 1095–1107.
[45] P. Shen, Z. Jiao, J.S. Zheng, W.F. Xu, S.Y. Zhang, A. Qin, et al., Injecting vascular endothelial growth factor into the temporomandibular joint induces osteoarthritis in mice, Sci. Rep. 5 (2015) 16244.
[46] K. Takayama, Y. Kawakami, M. Kobayashi, N. Greco, J.H. Cummins, T. Matsushita, et al., Local intra-articular injection of rapamycin delays articular cartilage degeneration in a murine model of osteoarthritis, Arthritis Res. Ther. 16 (2014) 482.